Supplemental Methods

RNAi screening
A minimum of 50-fold coverage of shRNA libraries was maintained at each step with the exception of the pre-treatment blood samples, which were limited in size and were at 20- to 40-fold coverage Final infection percentage of the library in leukemia cells was 5 – 10%. The average number of sequencing reads mapped to the 20K pool was 19 million.

GFP competition assays
Hairpins were validated using GFP competition assays by infecting a pure population of tdTomato or E2Crimson positive leukemia cells at 40 – 50% with single constructs expressing GFP and the shRNA of interest. 10^6 cells were injected into non-irradiated, syngeneic mice 48-72 hours after infection, and the GFP percentage at injection was measured using flow cytometry. Pre- and post-treatment samples were collected as in the screen; dasatinib (20 mg/kg) or vehicle was given 3 days q.d. (once per day) starting 11 days post-transplant for *in vivo* studies and for 3 days at 1 nM (LD~ 50 for 3 days treatment) starting five days post-plating for *in vitro* studies. GFP percentage was assessed at pre- and post-treatment by flow cytometric analysis. cDNA competition assays were performed similarly on tdTomato positive clonal populations with *Pafah1b3* wild type or *Pafah1b3* knockout backgrounds, using the *Pafah1b3* cDNA or an empty vector control in place of the shRNA. For survival studies, only 10^4 cells were injected per mouse, and drug dosing was performed as described in figures and figure legends.

Independent Component Analysis
Utilizing input data consisting of a hairpins-samples count matrix, ICA uses higher order moments to characterize the dataset as a linear combination of statistically independent latent variables. These latent variables represent independent components based on maximizing non-gaussianity, and can be interpreted as independent source signals that have been mixed together to form the dataset under consideration. Each component includes a weight assignment to each hairpin that quantifies its contribution to that component. Additionally, ICA derives a mixing matrix that describes the contribution of each sample towards the signal embodied in each component. This mixing matrix can be used to select signatures among components with distinct hairpin representation profiles across the set of samples.

Supplemental Tables

Supplemental Table S1. Primer sequences used for hairpin amplification and barcoding in in vivo and in vitro screens. To ensure that two mutations would be required to change the barcode of one sample to another functional barcode, the unmutated primers are not used.

5' unmutated primer
NNNNNTAGTGAAGCCACAGATGTA
5' primers with one basepair mutation to mark individual samples
NNNNNTAGTGACGCCACAGATGTA
NNNNNTAGTGAAGCCACCGATGTA
NNNNNTAGTGAGGCCACAGATGTA
NNNNNTAGTGAAGCCACGGATGTA
NNNNNTAGTGAAGCCGCAGATGTA
NNNNNTAGTGAAGCCACAGCTGTA
NNNNNTAGTGAAGCCACAGGTGTA
NNNNNTAGGGAAGCCACAGATGTA
3' unmutated primer
NNNNTTGAATTCCGAGGCAGTAGG
3' primers with one basepair mutation to mark individual samples

NNNNTTGCATTCCGAGGCAGTAGG
NNNNTTGGATTCCGAGGCAGTAGG
NNNNTTGACTTCCGAGGCAGTAGG
NNNNTTGAGTTCCGAGGCAGTAGG
NNNNTTGAATTCCGAGGCGGTAGG
NNNNTTGAATTCCGCGGCAGTAGG
NNNNTTGAACTCCGAGGCAGTAGG
NNNNTTGAAGTCCGAGGCAGTAGG

Supplemental Table S2. Genetic loci targeted by hairpins that have a Z-score < -2 for IC10. The RefSeq accession number, unique gene identifier (if available), and Z-score for component 10 are shown. Hairpins targeting these genes are predicted by ICA to enrich after dasatinib therapy *in vivo*.

Accession #	**Gene ID**	**Z-score (IC10)**
AC147806.5		-4.95
AC124202.3		-4.52
NM_177865	OTTMUSG00000008540	-4.42
NM_009644	Ahrr	-4.20
NM_194357	Rya3	-4.03
AK137052.1		-4.02
CT009738.8		-3.96
AK087644.1		-3.95
NM_026844	2310061C15Rik	-3.81
AC090869.7		-3.80

NM_001013024	Usp13	-3.78
NM_009619	Adam3	-3.65
NM_172415	Arhgef10l	-3.65
NM_145575	Cald1	-3.62
NM_181414	Pik3c3	-3.58
NM_026674	Aph1c	-3.55
NM_029186	Tmem180	-3.55
NM_146642	Olfr1140	-3.53
AC163615.5		-3.50
NM_146691	Olfr1467	-3.43
NM_028198	Xpo5	-3.40
NM_175021.3	Samd4b	-3.37
NM_173789	Helt	-3.37
NM_001081391	Csmd3	-3.37
NM_145450	BC022687	-3.34
AC158549.8		-3.34
NM_001009949	Mcart1	-3.33
NM_181275	Tas2r139	-3.31
NM_010290	Gja9	-3.31
AL626770.9		-3.30
AC125217.3		-3.24
AL603907.12		-3.21
NM_172445	Wdr37	-3.20

NM_026918	1810010M01Rik	-3.19
AC099884.12		-3.18
NM_172470	Wdr35	-3.16
NM_145476	Tbc1d22a	-3.15
AC134908.5		-3.15
AC107756.9		-3.14
NM_175130	Trpm4	-3.13
NM_175218	4930544M13Rik	-3.12
NM_145126	Chi3l4	-3.11
NM_146163	-	-3.09
NM_001163425.1	Myeov2	-3.09
AC159888.2		-3.07
NM_030715	Polh	-3.06
NM_177293	Mtap7d3	-3.03
AC132317.2		-3.03
NM_178224	Cbs	-3.02
NM_177075	C030019I05Rik	-3.02
NM_024236	Qdpr	-3.02
AK016124.1		-3.02
NM_175170	Pogk	-3.02
NM_030715	Polh	-3.00
NM_133910	Tbc1d14	-3.00
NM_145538	AI840826	-2.98

AC109140.6		-2.96
NM_146110	Aamp	-2.96
NM_172585	Larp5	-2.96
NM_001029867	Ugt2b36	-2.95
NM_178734	Zfp473	-2.95
AK034494.1		-2.95
NM_144925	Tnrc6a	-2.94
NM_145548	Cyp2j13	-2.94
NM_025338	Aurkaip1	-2.92
NM_198059	Nrap	-2.91
NM_198170	BC059842	-2.91
NM_177081	Ptpn7	-2.88
NM_172477	Dennd2a	-2.88
AC102693.9		-2.88
NM_026592	B230118H07Rik	-2.87
NM_133789	Strn4	-2.87
NM_027995	Paqr7	-2.87
AC161754.4		-2.85
AL844181.9		-2.83
NM_172684	Rsbn1	-2.83
AC122895.5		-2.83
NM_026812	Hddc3	-2.82
NM_199153	Tas2r102	-2.82

NM_146256	Hpdl	-2.82
NM_020576	Psors1c2	-2.80
AC153486.6		-2.79
NM_183281	2310005G13Rik	-2.79
NM_175443	Etnk2	-2.78
NM_001014997	Gm156	-2.78
NM_024473	BC005537	-2.77
NM_001042501	5830415L20Rik	-2.77
NM_133792	Lypla3	-2.77
NG_002057.2		-2.76
NM_028643	Efha1	-2.75
NM_017382	Rab11a	-2.75
AC122117.10		-2.74
NM_172521	Nut	-2.74
NM_016813	Nxf1	-2.73
NM_175682	9930021D14Rik	-2.73
AC121874.2		-2.73
NM_027807	Cul5	-2.73
NM_026255	Slc25a26	-2.72
NM_001029937	Sec14l3	-2.72
BC080301.1		-2.71
AC135861.5		-2.71
AC026767.30		-2.70

NM_001082476	Ndor1	-2.69
NM_145473	Csdc2	-2.68
BN000872.1		-2.68
NM_010196	Fga	-2.67
NM_027144	Arhgef12	-2.66
NM_021397	Zbtb32	-2.66
AC121579.3		-2.66
NM_028274	Exosc6	-2.65
NM_198637	1700016K19Rik	-2.65
NM_178220	Arrb1	-2.64
NM_027175	Ndufaf1	-2.64
AC098709.3		-2.63
NM_029297	Dynlrb2	-2.62
NM_177393	Vgcnl1	-2.61
NM_153398	Zbtb24	-2.61
NM_172303	Phf17	-2.61
AC102150.10		-2.61
NM_029253.1	Atf7ip2	-2.61
NM_147090	-	-2.61
NM_146288	Olfr122	-2.61
NM_144837	-	-2.60
NM_133996	Apon	-2.60
NM_174868	C030011O14Rik	-2.59

NM_148938	Slc1a3	-2.59
AC121826.3		-2.58
NM_001002239	Rpl17	-2.58
NG_007240.1		-2.58
NM_025659	Abi3	-2.58
NM_172453	Pif1	-2.57
NM_001141922.1	Bean1	-2.57
AK019736.1		-2.57
NM_028430.1	Ppil6	-2.57
NM_175096	D5Ertd593e	-2.56
NM_201405	Btnl1	-2.56
NM_028064	Slc39a4	-2.55
NM_153144	Ggnbp2	-2.55
NM_025910	Mina	-2.55
NM_025280	Kin	-2.55
NM_001033435	Gm885	-2.55
NM_001038015	Gnpda2	-2.55
NM_028534	Smap1	-2.55
AC123807.4		-2.55
NM_145433	Mrm1	-2.54
AC125045.4		-2.54
NM_007978	F8a	-2.54
NM_001164580.1	BC030336	-2.53

NM_001004142.2	Nlrp1a	-2.51
NG_012988.1		-2.51
NG_001704.2		-2.51
NM_134134	A630042L21Rik	-2.49
NM_172609	Tomm22	-2.49
NM_175343	Chdh	-2.49
AC158586.8		-2.48
AC009725.12		-2.45
NM_146414	Olfr1431	-2.45
NM_008866	Lypla1	-2.45
NM_019770	Tmed2	-2.44
BX649260.4		-2.44
NM_147053	Olfr582	-2.44
AC154374.1		-2.44
NM_145513	Tiprl	-2.44
NM_177244	Fastkd1	-2.43
NM_178017	Hmgb2l1	-2.43
NM_025343	Rmnd1	-2.43
XR_105165.1	B130055M24Rik	-2.43
NM_080440	Slc8a3	-2.43
NM_172601	Rab2b	-2.42
AC152398.7		-2.42
AC154395.4		-2.41

NM_130865	Atx	-2.41
AC112261.4		-2.40
NM_145416	BC021438	-2.40
NM_175315.1	Ceacam15	-2.40
NM_173766	A630023P12Rik	-2.40
NM_173427	Klhdc7a	-2.40
NM_027395.2	Basp1	-2.40
NM_133350	Mapre3	-2.40
NM_010211	Fhl1	-2.40
NM_146494	Olfr722	-2.40
NM_145938	Rpp40	-2.40
NM_001025572	Ankrd12	-2.39
AC068911.38		-2.39
NM_016658	Galt	-2.39
NM_001081389	Nlrp6	-2.39
NM_134077	Rbm26	-2.38
NM_175297	-	-2.38
NG_018374.1		-2.38
AL627349.8		-2.38
NM_177355	Plcxd3	-2.37
NM_001033149	Ttc9	-2.37
NM_147029	Olfr1120	-2.35
AC158388.2		-2.34

XM_001477076.2	LOC675594	-2.34
AL844208.5		-2.34
NM_144818	Ncaph	-2.33
NR_033538.1		-2.33
NM_172722	C330023M02Rik	-2.33
BX004985.6		-2.33
NM_024282	5830417C01Rik	-2.32
AC109183.17		-2.32
NM_007935	Epc1	-2.32
AC098886.4		-2.31
NM_177607	4933430I17Rik	-2.31
AC125373.4		-2.31
NM_177893	-	-2.31
NM_007756	Cplx1	-2.31
AK036683.1		-2.30
NM_020252	Nrxn1	-2.30
AC124520.4		-2.30
AC108915.12		-2.29
NM_027353	Cd2bp2	-2.29
AK043809.1		-2.29
NM_146079	Guca1b	-2.29
NM_001013376	Rpp38	-2.28
NM_027904.3	Cpn2	-2.28

NM_181819.2	Wfikkn2	-2.27
NM_001018031	Gm414	-2.27
NM_175448	A330019N05Rik	-2.27
NM_019763	Spen	-2.27
NM_177608	3110001I20Rik	-2.27
NM_026385	Pllp	-2.27
NM_001081157	Lmod3	-2.27
NM_177697	E030013G06Rik	-2.27
NM_146218	Rfwd3	-2.26
CT030197.14		-2.26
NM_009521	Wnt3	-2.26
NG_017822.1		-2.25
AC131084.13		-2.25
NM_013475	Apoh	-2.25
NM_146646	Olfr152	-2.25
NM_001081653.1	Cntnap5c	-2.24
AC114003.4		-2.24
AC099625.11		-2.24
BC042508.1		-2.24
NM_145401	Prkag2	-2.24
NM_025504	2310004L02Rik	-2.23
NM_138590	-	-2.23
NM_023699	Nfatc4	-2.23

NM_016716	Cul3	-2.23
NM_177913	A430089I19Rik	-2.23
NM_177904	6030452D12Rik	-2.23
NM_001163136.1	Macc1	-2.23
NM_026547.1	1520402A15Rik	-2.23
NM_172937	Shprh	-2.23
NM_028820	1700017B05Rik	-2.23
NM_177380	Cyp3a44	-2.22
AC126276.3		-2.22
NG_018731.1		-2.22
NM_146768	Olfr1099	-2.22
NM_001001335	Plekha8	-2.22
AC138214.8		-2.22
NM_178771	Klhl26	-2.22
NM_001033454	AI427809	-2.21
NM_175325	Bbs4	-2.21
NM_001011775	Olfr1419	-2.20
NM_012052	Rps3	-2.20
BX842660.2		-2.20
NM_027493	Actr8	-2.20
BC006792.1		-2.20
AC104139.6		-2.20
AL928998.9		-2.20

AL589737.11		-2.20
AK138212.1		-2.20
BK000964.1		-2.20
AC154463.2		-2.20
NM_177829	Spink10	-2.20
AL732417.19		-2.19
NM_146223	Cplx3	-2.19
NM_183016	Cdc42bpb	-2.19
NM_146567	Olfr843	-2.19
AL672244.15		-2.19
NG_005612.1		-2.18
NM_012015	H2afy	-2.18
NM_001013025	Tgfbrap1	-2.18
NM_138658	Gnas	-2.18
AC107711.13		-2.17
BC108341.1		-2.17
NM_172786	Il20ra	-2.17
AL670292.9		-2.17
NM_019583	Il17rb	-2.17
NM_023526	Nkiras1	-2.16
NM_026521	Zfp706	-2.16
NM_146485	Olfr183	-2.16
NM_177032	-	-2.15

NM_008474	Krt84	-2.15
NM_178901	AI467606	-2.15
NM_177059	Fstl4	-2.15
AC005992.15		-2.15
NM_027375	Gcc2	-2.15
NG_017806.1		-2.15
NM_207527	4930504O13Rik	-2.15
NM_026465	2010316F05Rik	-2.15
NM_008367	Il2ra	-2.14
NM_001033348	A230067G21Rik	-2.14
NM_001029937	Sec14l3	-2.13
AC117797.9		-2.13
NM_009401	Tnfrsf8	-2.13
AC110235.13		-2.13
AK018099.1		-2.13
NM_133981	Alg9	-2.13
NM_130879	Usp48	-2.13
NM_029868	Gpbp1l1	-2.13
NG_019354.1		-2.13
AL731682.20		-2.12
NM_177025	Cobll1	-2.12
XM_003085666.1	4933406P04Rik	-2.12
NM_025362	Wbscr18	-2.12

NM_030553	Olfr160	-2.12
NM_022986	Irak1bp1	-2.12
AK021136.1		-2.12
AC121271.8		-2.12
AL808127.4		-2.11
AC114988.21		-2.11
NM_153528	Gramd1c	-2.11
NM_133697	1110003E01Rik	-2.11
NM_009738	Bche	-2.11
NM_026574	Inoc1	-2.11
AC109196.12		-2.11
NM_183098	1700084P21Rik	-2.10
NM_138594	D6Wsu163e	-2.09
AK017899.1		-2.09
NM_177389	Mia3	-2.09
AC145211.3		-2.09
NM_001081265	Heatr2	-2.09
NM_027013.2	Scnm1	-2.09
AC124568.3		-2.09
NM_013485	C9	-2.08
NM_001013376	Rpp38	-2.08
NM_001081977	Rnf144	-2.08
NM_023799	Mgea5	-2.07

AC159632.2		-2.07
NM_001003950	Rab3ip	-2.07
NG_020062.1		-2.07
NM_172528	Lrrc1	-2.07
AC155274.2		-2.07
AC087417.27		-2.07
NM_194342	Unc84b	-2.06
NG_007909.3		-2.06
AC119870.17		-2.06
NR_029414.1		-2.06
NM_013516	Ms4a2	-2.06
AC191865.3		-2.06
NM_026648	Lrrc50	-2.06
NM_010859	Myl3	-2.06
NM_028110	Dennd2d	-2.06
NM_030024	Prr15	-2.06
NM_173441	Iws1	-2.05
NM_022655	Ireb2	-2.05
CT025157.6		-2.05
NM_027230	Prkcbp1	-2.05
NM_001162933.1	Rpl10l	-2.05
AC133203.3		-2.05
NM_053228	V1rb7	-2.04

NM_001005358	BC018101	-2.04
AK007040.1		-2.04
NM_175358	Zdhhc15	-2.04
AC132414.4		-2.04
NM_178901	AI467606	-2.04
NM_009689	Birc5	-2.03
AC119810.8		-2.03
NM_175003	AU040829	-2.03
NM_016852	Wbp2	-2.03
NM_007420	Adrb2	-2.02
NM_172530	She	-2.02
NM_019988	Gbl	-2.02
NM_001029867	Ugt2b36	-2.01
AK139810.1		-2.01
NM_177234	B230340J04Rik	-2.01
NM_016716	Cul3	-2.01
AC153803.1		-2.01
AC113068.9		-2.01
NM_172616	C330027C09Rik	-2.01
AK156200.1		-2.01
NM_146423	Olfr887	-2.01
NM_024290	Tnfrsf23	-2.00
NM_153555	Wdr42a	-2.00

AC154224.1		-2.00

Supplemental Table S3. Genetic loci targeted by hairpins that have a Z-score > 2 for IC10. The RefSeq accession number, unique gene identifier (if available), and *Z*-score for component 10 are shown. Hairpins targeting these genes are predicted by ICA to deplete after dasatinib therapy *in vivo*.

Accession #	**Gene ID**	**Z-score (IC10)**
NM_001195255.1	Gm581	4.45
NM_175251	Arid2	3.93
AL805899.20		3.93
NM_134142	Tmem109	3.88
AC087799.43		3.52
NM_175246	Snip1	3.51
AK089806.1		3.50
NM_144815	Cecr5	3.48
AC130821.3		3.46
NM_011452	Serpinb9b	3.40
AC127173.17		3.40
NM_001039485.3	Fam38b	3.33
NM_016717	Scly	3.25
AK041457.1		3.24
BX664729.3		3.23
AK076377.1		3.23
NM_175263	5730593N15Rik	3.22
NM_001001335	Plekha8	3.22

NG_020660.1		3.20
NM_001003913	Mars	3.17
NM_007892	E2f5	3.16
NM_001002897.3	Atg9b	3.16
NM_009535	Yes1	3.14
NM_138630	Arhgap4	3.14
AK037912.1		3.14
NM_010228	Flt1	3.10
AC102232.12		3.10
NM_008169	Grin1	3.07
AC138739.8		3.07
AC130474.12		3.06
NM_009428	Trpc5	3.06
NM_177848	OTTMUSG00000015529	3.06
AC154367.1		3.05
NM_020503	Tas2r119	3.04
NM_010747	Lyn	3.03
NM_030166	Galntl2	3.02
NM_001085511.1	4932429P05Rik	3.01
XM_127665.6	9230112D13Rik	2.99
NM_172614	Tmem44	2.96
NM_024456	Rab5c	2.96
NM_001081202	L1td1	2.96

NM_177060	9930039A11Rik	2.95
NM_001029936	Specc1	2.95
AC132408.2		2.92
XR_104808.1	Fam188b2	2.92
NM_001033235	Trim40	2.92
AC156798.2		2.92
NM_016872	Vamp5	2.91
NM_011890	Sgcb	2.89
NM_016959	Rps3a	2.88
NM_001044697	Zfp2	2.88
NM_173388	Slc43a2	2.87
NM_145590	BC017158	2.87
NG_002028.2		2.86
AL591854.18		2.85
NM_001099328.1	Zfp831	2.83
NG_012580.1		2.81
AC154558.2		2.81
NM_019685	Ruvbl1	2.81
NM_023814	Tbx18	2.80
NM_001033314	C530028I08Rik	2.79
NM_177009	Smyd4	2.77
NM_175441	D830007F02Rik	2.77
NM_146577	Olfr1043	2.76

NM_026128	4930403L05Rik	2.74
NM_029773	4921517N04Rik	2.74
NM_198619	MGC67181	2.73
NM_201369.3	N4bp2l2	2.72
NM_001101461.2	9130204L05Rik	2.72
NG_018204.1		2.71
NM_177661	C130079G13Rik	2.70
AC087116.13		2.70
NM_030701	Gpr109a	2.69
NM_025310	Ftsj3	2.68
NM_153591	Nars2	2.68
XR_106273.1	4933407E24Rik	2.68
NM_026522	Chid1	2.68
NM_146494	Olfr722	2.67
NM_020565	Sult3a1	2.67
XM_003084620.1	Ccdc149	2.66
NM_182995	6330503K22Rik	2.66
AL732456.6		2.64
AL929524.16		2.64
NM_183392	Nup54	2.64
AC155825.2		2.63
NM_011774	Slc30a4	2.63
NM_172793	Btnl9	2.63

NM_145139	Eif3s6ip	2.62
AC165969.5		2.62
NM_146179	Zfp418	2.61
NM_001081217	Zfp174	2.61
AC124553.4		2.61
NM_145985	Arcn1	2.60
NM_198967	Tmtc1	2.59
NM_177095	-	2.59
NM_025821	Carhsp1	2.59
XM_003084831.1	9130014G24Rik	2.59
BX649226.1		2.59
NM_175303	Sall4	2.58
AK052410.1		2.58
NM_001081287	Mpp7	2.58
AC154224.1		2.57
AC055817.12		2.57
AC156271.5		2.57
AK019125.1		2.57
AC156607.5		2.56
NM_001101478.1	D3Ertd254e	2.55
NM_177847	A730036I17Rik	2.55
NM_178734	Zfp473	2.54
NM_198001	1110008P14Rik	2.54

NM_010785	Mdm1	2.53
NM_027180	Centd2	2.53
XM_003084471.1	LOC100502613	2.53
AL929142.6		2.52
AK032662.1		2.52
AC122486.4		2.51
AC153377.5		2.51
XM_003085977.1	Gm8973	2.51
NM_130453	Gpha2	2.50
NM_146328	Olfr110	2.50
NM_007460	Ap3d1	2.49
AK078603.1		2.49
NM_146382	Olfr461	2.49
NM_008508	Lor	2.49
NM_010275	Gdnf	2.48
NM_172272	Pars2	2.47
NM_028030	Rbpms2	2.46
AL645797.11		2.46
NM_153546	Mboat1	2.46
NM_027338	Vps36	2.46
NM_027191	Nup37	2.46
NM_175134	Ankrd46	2.45
NM_031875	Otof	2.45

CT030722.6		2.45
NM_152821	Purg	2.45
NM_026467	Rps27l	2.44
NM_144517	Tbc1d19	2.43
AL627123.13		2.42
NG_018471.1		2.41
NM_145744	Dusp15	2.41
NM_027872	Slc46a3	2.40
NM_172937	Shprh	2.40
NM_001081204	B3galtl	2.40
NM_146186	-	2.40
NM_144790	Ankrd33	2.40
NG_012017.1		2.40
NM_152813	Plcd3	2.39
NM_146350	Olfr1123	2.39
NM_175259	Tmem58	2.38
AK028613.1		2.38
NM_024180	Ormdl2	2.38
AC139572.4		2.38
NM_177150	Cenpt	2.37
NM_198034	Sidt1	2.36
AC105905.10		2.36
NM_016889	Insm1	2.36

NM_146451	Olfr164	2.36
NM_133724	Cno	2.35
NM_020252	Nrxn1	2.35
AA682037	Rps6kc1	2.35
NM_175693	-	2.34
NM_020521	V1rb5	2.34
AC102430.9		2.34
NM_019988	Gbl	2.34
AC130821.3		2.34
AC107758.19		2.34
NM_172770	Ttc12	2.33
AC154640.2		2.33
NM_010147	Epn1	2.32
NM_028030	Rbpms2	2.32
NM_175347	Srl	2.32
NM_021389	Sh3kbp1	2.32
AK006663.1		2.32
NM_001081306	Ptprz1	2.31
NM_001013755	5730409E04Rik	2.31
AC119177.11		2.31
AC139241.4		2.30
NM_016982	Vpreb1	2.30
AK034470.1		2.30

NM_009462	Usp10	2.30
NM_011807	Dlg2	2.30
NM_010136	Eomes	2.30
AC124533.4		2.30
NM_054077	Prelp	2.30
NM_027698	Exod1	2.29
NM_011920	Abcg2	2.29
NM_008592	Foxc1	2.29
NM_134192	V1re3	2.29
AC121832.3		2.29
NM_001081247	Polr3a	2.29
NM_001126316.1	Gm438	2.29
NM_177697	E030013G06Rik	2.28
NM_010154.1	Erbb4	2.28
NM_027121	Vkorc1l1	2.28
AL929413.13		2.28
NM_146261	BC031748	2.28
AK040340.1		2.28
NM_145550	Yipf1	2.28
NM_177624	A430083B19Rik	2.27
NM_001081391	Csmd3	2.27
NM_177471	Ccdc69	2.27
AL589876.11		2.27

NM_172740	-	2.27
NM_026886	1500001A10Rik	2.27
NM_134469	Fdps	2.26
AC133090.4		2.26
AB116374.1		2.26
NM_144920	Plekha5	2.26
XM_137324.3	Gm4801	2.25
NM_015733	Casp9	2.25
AC122818.4		2.24
AC108777.7		2.24
NM_146306	Olfr518	2.23
NM_016796	Vamp4	2.23
AC114998.13		2.23
NM_008776	Pafah1b3	2.23
NM_178402	-	2.23
NM_026438	Ppa1	2.23
AC109281.5		2.23
AC152951.2		2.23
NM_198671	Gse1	2.22
NM_018739	rp9	2.22
NM_001081080	Phf3	2.22
NG_020564.1		2.22
NG_018172.1		2.21

AC154451.2		2.21
NM_001003919	Ddx11	2.21
AC124765.2		2.21
NM_053008	Olig3	2.21
NG_019793.1		2.20
NM_182930	Plekha6	2.19
NM_177622	A230042K10Rik	2.19
NM_153564	Gbp2	2.19
NM_133905	Papd4	2.19
AC124742.4		2.18
NM_080638	Mvp	2.18
NM_009254	Serpinb6a	2.18
NM_019951	Sec11a	2.18
NM_177471	Ccdc69	2.17
NM_177264	9230112E08Rik	2.17
AC132612.3		2.17
AC107811.28		2.17
NM_029491	D030074E01Rik	2.17
NM_007925	Eln	2.17
NM_177290	Itgb8	2.17
AC114547.12		2.17
AC159476.5		2.17
NG_018964.1		2.16

NM_010705	Lgals3	2.16
NG_019793.1		2.16
AC154872.10		2.16
AC101221.12		2.16
NM_172721	Fbxw8	2.16
NM_028134	Lysmd1	2.16
NM_009968	Cryz	2.16
NM_030718	Abo	2.16
NM_029884	Hgsnat	2.15
NM_026785	Ube2c	2.15
NM_009917	Ccr5	2.15
AK020104.1		2.15
NM_025814	Serbp1	2.15
NG_018021.1		2.15
NM_027547	Prdm5	2.15
AK086549.1		2.15
NM_177098	4930412M03Rik	2.14
NM_012022	Ppnr	2.14
NM_172607	Naprt1	2.14
NM_130856	Krtap16-8	2.14
AC139349.4		2.14
NM_133954	AA960436	2.14
NM_023813	Camk2d	2.14

NM_175254	9330180L21Rik	2.14
NM_175317	Eftud1	2.13
NM_146409	Olfr1080	2.12
NM_001080931	Thrap1	2.12
AK006847.1		2.12
NM_211138	Pcyt1b	2.12
NM_145491	Rhoq	2.11
AC115805.12		2.11
NM_177192	D030011O10Rik	2.11
NM_009686	Apbb2	2.11
NM_011857	Odz3	2.11
NM_031493	Xlr5c	2.11
NM_175540	Eda2r	2.11
NM_032400	Sucnr1	2.11
NM_026083	Zc3h13	2.11
NM_001081111	Tmf1	2.11
AC153597.13		2.11
NM_008698	Nipsnap1	2.11
NM_172264	Chdh	2.10
NM_173865	Slc41a1	2.10
AC161246.2		2.10
NM_001085500.2	Cisd3	2.10
NM_001099277.1	Zfp541	2.10

NM_177326	Pak2	2.10
NM_153803	BC038479	2.10
NM_001159942.1	Plekhg1	2.09
NM_021446	0610007P14Rik	2.09
AK017517.1		2.09
NG_007741.3		2.09
NM_010082	Adam28	2.09
NM_053170	Trim33	2.08
NM_026866	Disp1	2.08
NM_021326	Rbak	2.08
AC114924.5		2.08
NM_024444	Cyp4f18	2.08
NM_001001319	Pramel4	2.08
NM_146152	Ipo13	2.08
NM_134123	-	2.08
AC126943.5		2.08
NM_138753	Hexim1	2.07
NM_178243	5830403L16Rik	2.07
NM_011200	Ptp4a1	2.07
NM_016799	Srrm1	2.07
AC098875.3		2.07
NM_001081059	Ccdc90a	2.06
AC116386.9		2.06

AC119842.9		2.06
NM_182928	Adm2	2.06
NG_006498.2		2.06
AC060761.10		2.06
NM_001081191	Eml5	2.06
NM_173771	4933406M09Rik	2.05
NM_134077	Rbm26	2.05
AK020394.1		2.05
AC118642.11		2.05
NM_029707	1700023I07Rik	2.05
AC125223.3		2.05
NM_019419	Arl6ip1	2.05
NM_172740	-	2.05
AC132305.3		2.05
NM_009459	Ube2h	2.05
NM_021455	Mlxipl	2.04
AC122251.4		2.04
NM_146126	Sord	2.04
NM_145402	Tmem51	2.04
AC164290.4		2.04
NM_130450	Elovl6	2.04
AL773540.18		2.04
NM_024237	1600015H20Rik	2.04

NM_019776	Snd1	2.03
NM_021319	Pglyrp2	2.03
NM_001111317.1	BC048609	2.03
NM_175381	2700081O15Rik	2.03
NM_001003915	Slc5a12	2.03
NM_152811	Ugt2b1	2.03
NM_172683	Pogz	2.03
AC129180.3		2.03
NM_172935	Amdhd2	2.03
AK089280.1		2.03
AC135861.5		2.02
NM_026776	Vps25	2.02
NM_146359	Olfr564	2.02
NM_145460	Oxnad1	2.02
NM_133917	Mlxip	2.02
NM_009734	Azi1	2.02
NG_020439.1		2.02
NM_001040434.1	Rgag1	2.02
AC157521.2		2.02
NM_146311	Olfr510	2.01
NM_145921	Olah	2.01
NM_146543	Olfr1360	2.01
NM_024478	Grpel1	2.01

AK006834.1		2.01
NM_177292	C530024P05Rik	2.01
NM_001029979	Safb2	2.01
AK030544.1		2.01
AC153512.2		2.01
NM_053156	Allc	2.01
AC025586.4		2.00
NM_133791	Wwc2	2.00
NM_028111	2010109K11Rik	2.00
NM_001033535	Tnfaip8l3	2.00
AC117635.6		2.00

Supplemental Figures

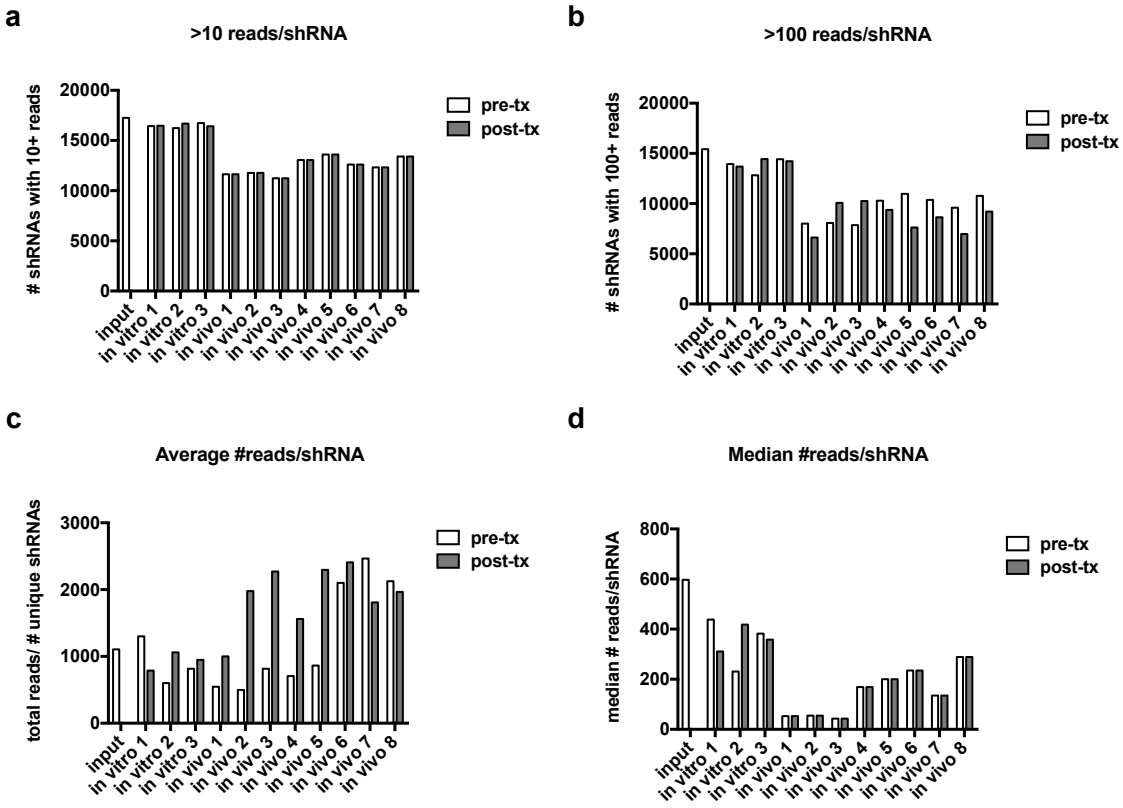

Supplemental Figure S1. shRNA representation in in vivo and in vitro screens. Bar graphs showing the number of shRNAs with at least 10 reads/shRNA (top left), at least 100 reads/shRNA (top right), the mean number of reads/shRNA (bottom left), and the median number of reads/shRNA (bottom right) from raw *in vivo* and *in vitro* screening data.

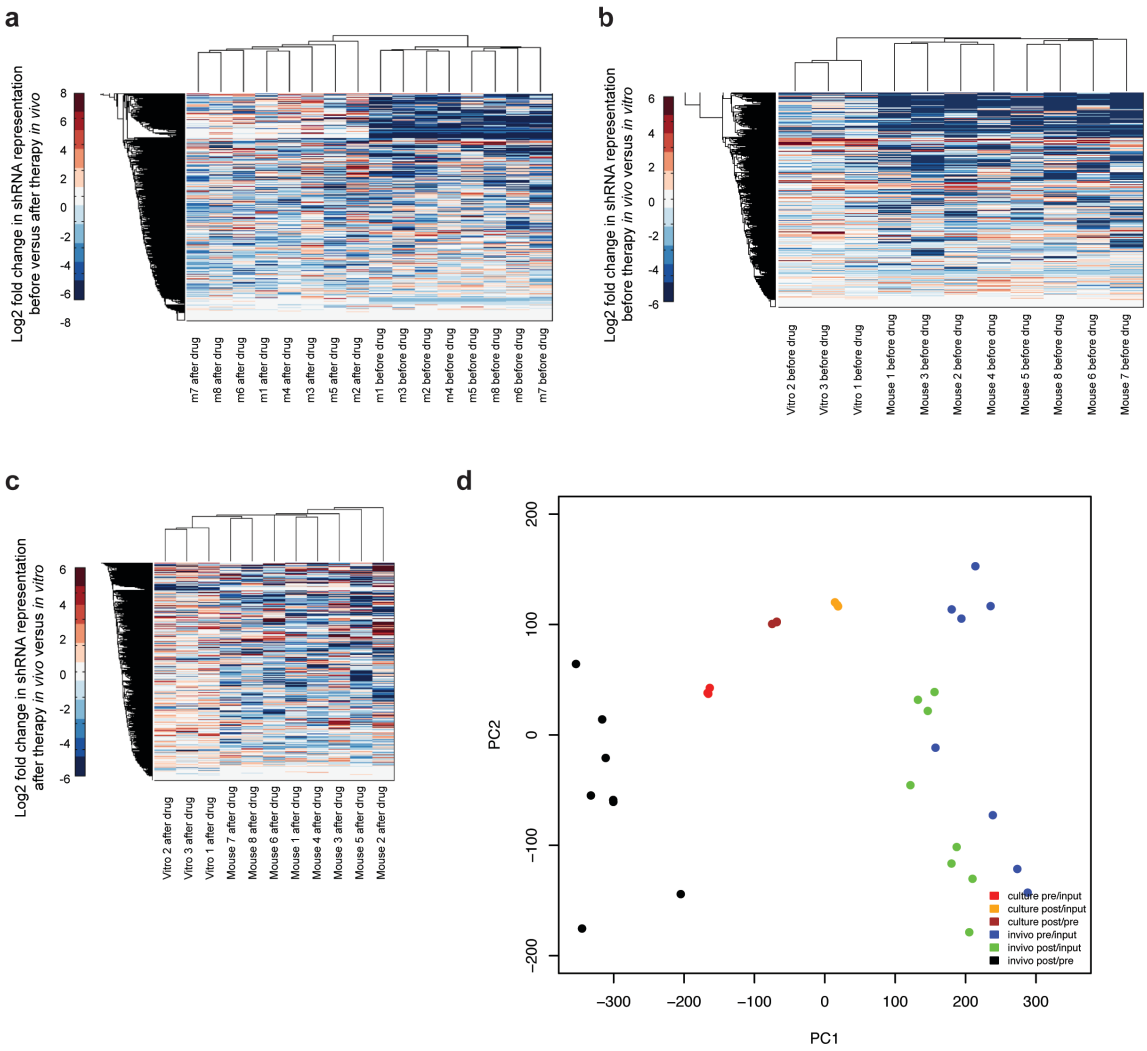

Supplemental Figure S2. Hierarchical clustering separates pre- and post-treament samples as well as samples from in vivo vs in vitro screens.
(a) Hierarchical clustering of $\log_2$ fold change in shRNA representation before vs after therapy shows that hairpins have distinct behavior before dasatinib vs after *in vivo*. (b) and (c) Hierarchical clustering of $\log_2$ fold change in shRNA representation *in vivo* vs *in vitro* during period (b) before treatment shows that hairpins have distinct behavior *in vivo* during general leukemia progression, and (c) during and after treatment shows that hairpins have distinct behavior *in vivo* during therapeutic response. (d) Principal component analysis of $\log_2$ fold changes before (pre/input) and after treatment (post/pre) as well as over the entire screening period (post/input) *in vivo* and *in vitro* shows that while the post/input fold change *in vitro* forms a distinct cluster, the post/input fold change *in vivo* clusters with the before treatment samples, indicating that hairpin behavior *in vivo* is primarily defined by sample-specific effects between different mice.

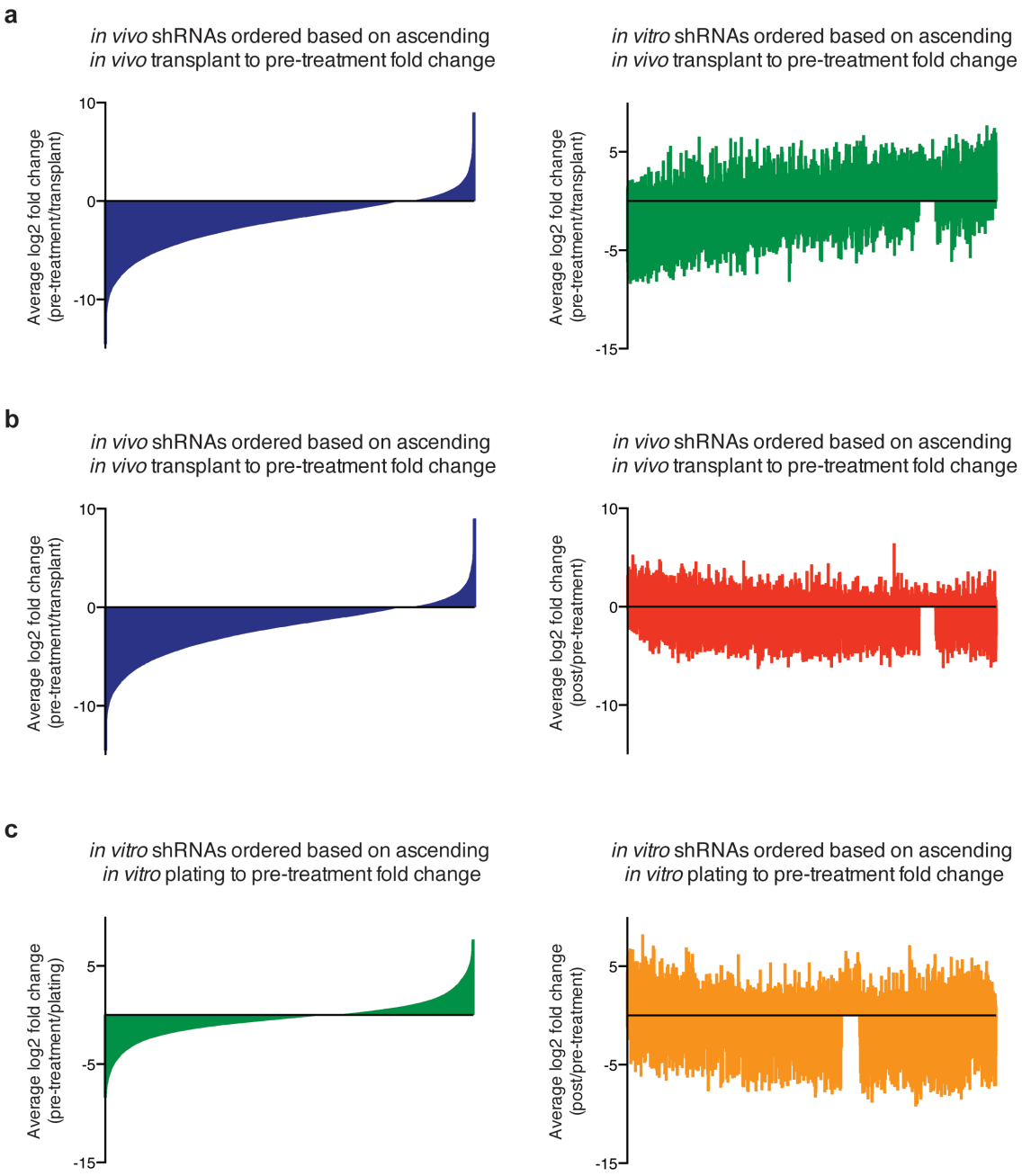

Supplemental Figure S3. Limited mutual information exists in hairpin behavior before versus after therapy as well as in vivo as compared to in vitro.
(a) Waterfall plots representing the $\log_2$ fold changes before dasatinib therapy of all shRNAs in the library *in vivo* (blue) and *in vitro* (green), with shRNAs arranged in rank ascending order based on their $\log_2$ fold change *in vivo*. Hairpin behavior *in vivo* does not predict behavior *in vitro* before therapy. (b) Waterfall plots representing the $\log_2$ fold changes *in vivo* of all shRNAs in the library before therapy (blue) and after therapy (red), with shRNAs arranged in rank ascending order based on their $\log_2$ fold change *in vivo* before therapy. Hairpin behavior before therapy does not predict behavior after therapy *in vivo*. (c) Waterfall plots representing the $\log_2$ fold changes *in vitro* of all shRNAs in the library before

therapy (green) and after therapy (orange), with shRNAs arranged in rank ascending order based on their $\log_2$ fold change *in vitro* before therapy. Hairpin behavior before therapy does not predict behavior after therapy *in vitro*.

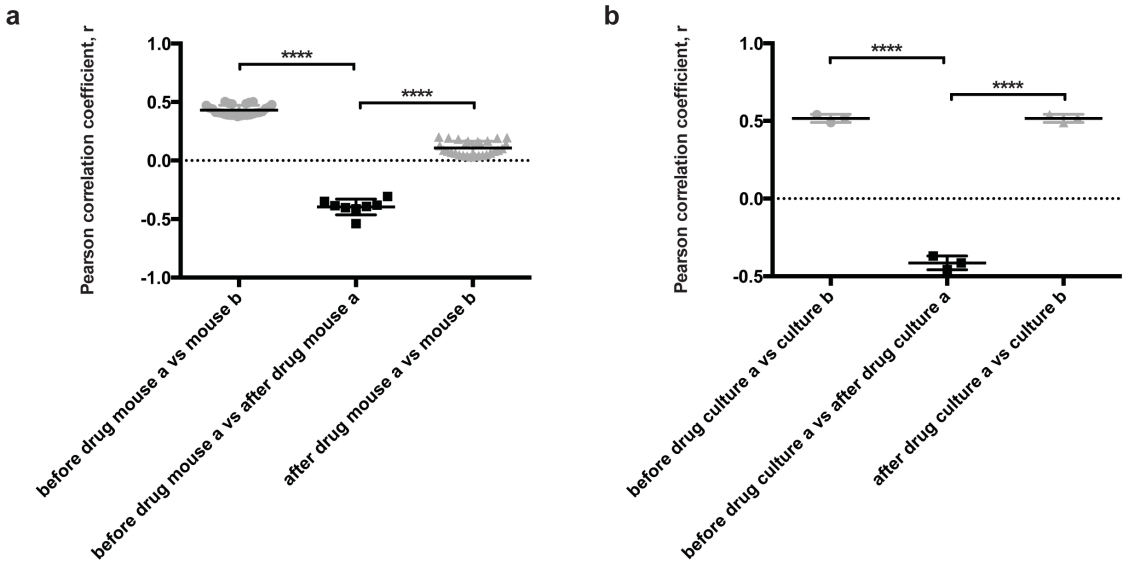

Supplemental Figure S4. Correlation between biological replicates in longitudinal RNAi screen is significantly higher than between non-replicates.
(a) Scatterplot showing Pearson correlation coefficients of $\log_2$ fold changes *in vivo* of all shRNAs in library between biological replicates (grey) as compared to non-replicates (black). (b) Scatterplot showing Pearson correlation coefficients of $\log_2$ fold changes *in vitro* of all shRNAs in library between biological replicates (grey) as compared to non-replicates (black). Biological replicates are significantly more correlated to each other than they are to non-replicate samples (different setting or therapeutic context), indicating that hairpin behavior is not occurring randomly. Error bars represent standard deviation; p-values were calculated using Student's t-test.

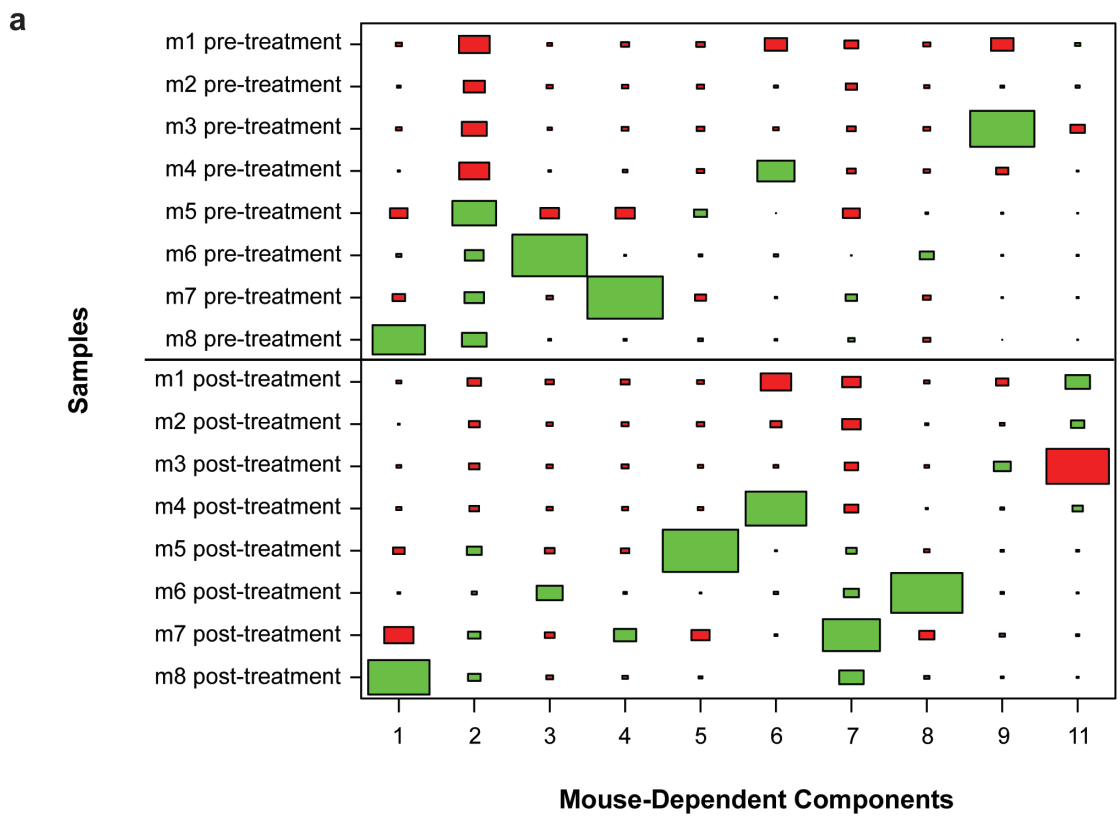
a
m1 pre-treatment
m2 pre-treatment
m3 pre-treatment
m4 pre-treatment
m5 pre-treatment
m6 pre-treatment
m7 pre-treatment
m8 pre-treatment
m1 post-treatment
m2 post-treatment
m3 post-treatment
m4 post-treatment
m5 post-treatment
m6 post-treatment
m7 post-treatment
m8 post-treatment
Samples
1
2
3
4
5
6
7
8
9
11
Mouse-Dependent Components

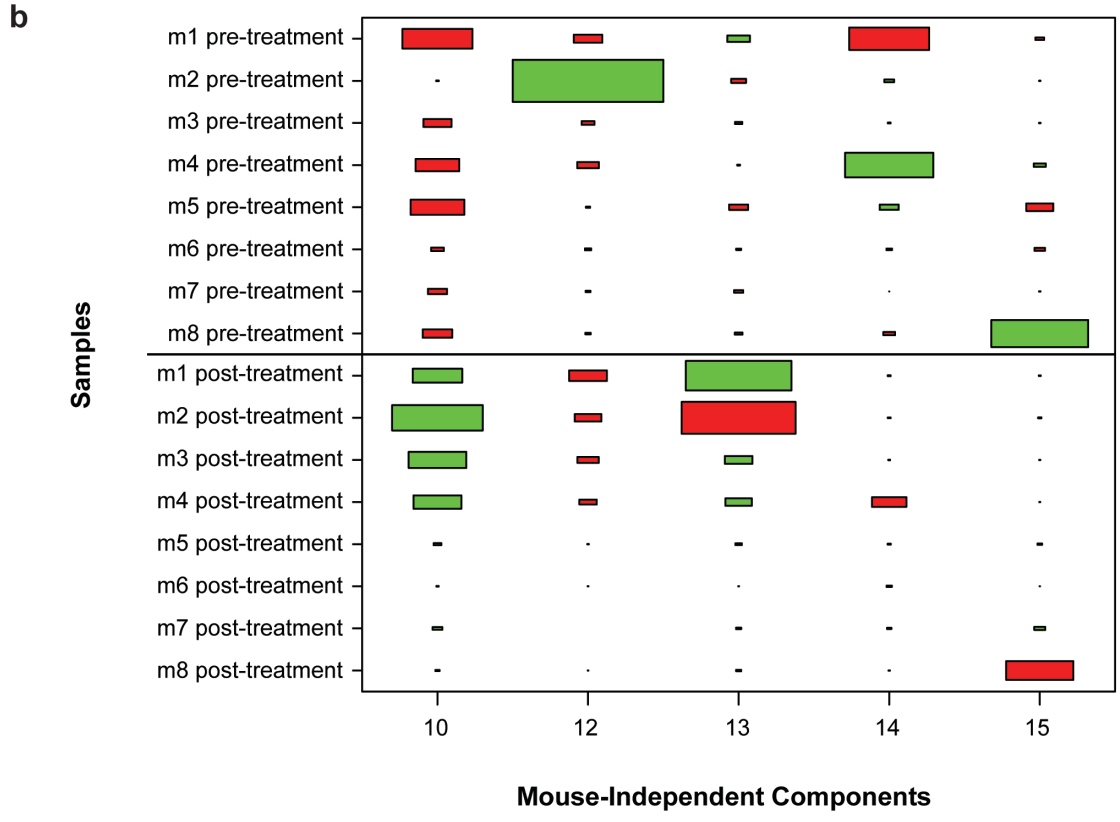
b
m1 pre-treatment
m2 pre-treatment
m3 pre-treatment
m4 pre-treatment
m5 pre-treatment
m6 pre-treatment
m7 pre-treatment
m8 pre-treatment
m1 post-treatment
m2 post-treatment
m3 post-treatment
m4 post-treatment
m5 post-treatment
m6 post-treatment
m7 post-treatment
m8 post-treatment
Samples
10
12
13
14
15
Mouse-Independent Components

Supplemental Figure S5. Independent component analysis of longitudinal in vivo RNAi screening data isolates mouse-dependent and mouse-independent signatures. (A) and (B) Hinton plots of independent components show the signature generated by each mouse-dependent (A) or mouse-independent (B) component across all *in vivo* samples before and after dasatinib treatment. Colors represent the directionality of hairpin representation (red enriched, green depleted), and the size of each rectangle quantifies the strength of the signature for that sample. Each component identifies a two-sided signature, such that there are enriched and depleted hairpins within each sample for each signature; components are numbered according to their original identification in the ICA.

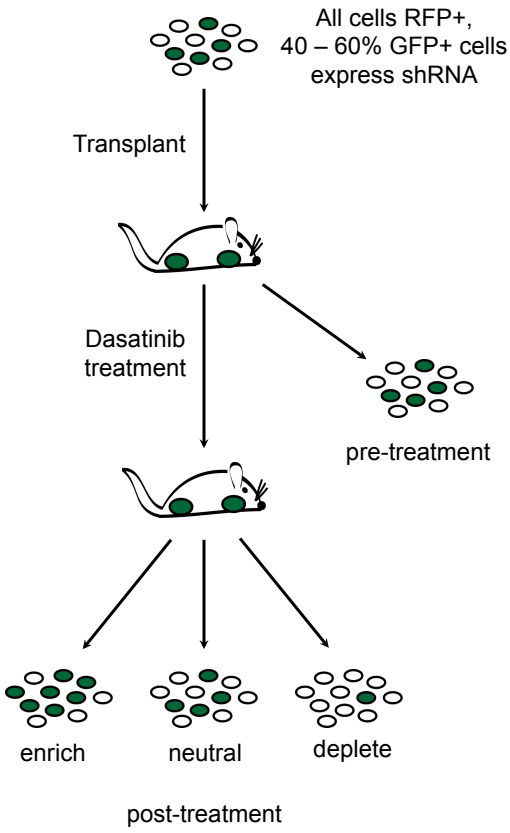

Supplemental Figure S6. Schematic for GFP competition assays. Leukemia cells (background labeled with tdTomato or E2Crimson) are partially transduced with a construct containing GFP and the shRNA of interest, and cells are then transplanted into recipient mice (10^6 cells/mouse) or plated *in vitro* as in the screen. Mice were treated with 20 mg/kg dasatinib for 3 days q.d. starting 11 days post-injection; cells were treated with 1 nM dasatinib for 3 days. Higher doses are used than in the screen, as we do not have to maintain as high of complexity when using single constructs. At transplant, pre-, and post-treatment, the percentage of shRNA-expressing cells is assessed by flow cytometric analysis, and fold change of % shRNA-expressing cells over time can be calculated. An empty vector or shRNA against Renilla luciferase, which these cells do not express, are used as negative controls; a hairpin against *Abl1*, which should have significantly different representation before versus after therapy, is used as a positive control.

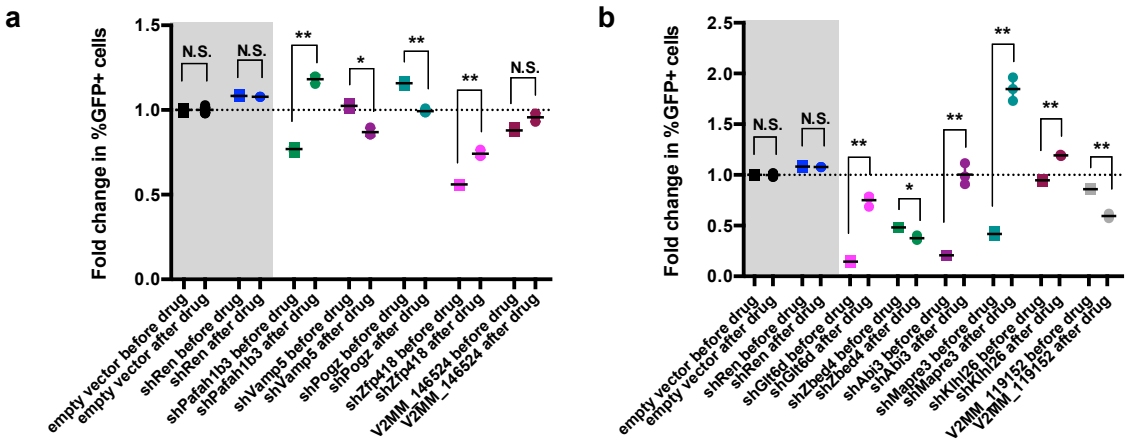

Supplemental Figure S7. In vitro validation of shRNAs predicted to enrich or deplete by GFP competition assay. (a) and (b) Scatterplots showing normalized fold change of shRNA-expressing cells before and after dasatinib treatment *in vitro* in GFP competition assays or hairpins predicted to deplete after therapy (a) or enrich after therapy (b) by IC10. Controls are in the grey box: an empty hairpin vector and a hairpin targeting Renilla luciferase are negative controls, and a hairpin targeting *Abl1*, which is the driving oncogene in these cells and the target of therapy, is included as a positive control of an shRNA that has significantly different fold change before versus after therapy. Fold changes are normalized to an empty vector or a hairpin targeting Renilla luciferase, which these cells do not express. Error bars represent standard deviation; p-values were calculated using Student's t-test.

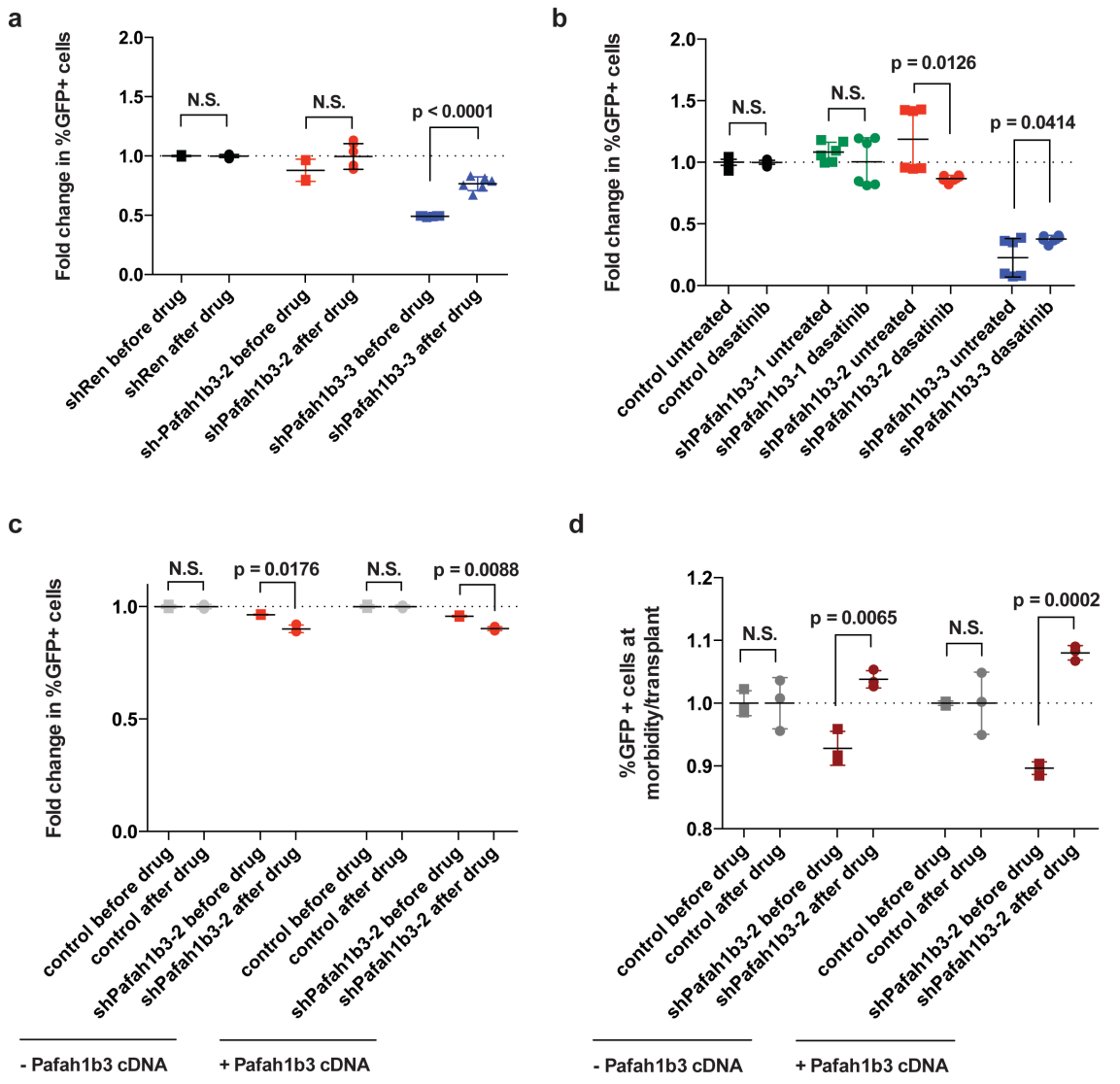

Supplemental Figure S8. Pafah1b3 loss sensitizes cells to dasatinib in vivo but not in vitro. (a) Scatterplot showing fold change in percent shRNA-expressing cells before versus after dasatinib therapy *in vitro* of additional *Pafah1b3* hairpins that cannot target the *Pafah1b3* cDNA. An shRNA targeting Renilla luciferase, which is not expressed by these cells, is used as a control. (b) Scatterplot showing fold change in percent shRNA-expressing cells of all three *Pafah1b3* shRNAs in both untreated and dasatinib-treated cultures. shPafah1b3-1 targets the coding region of the gene and thus the cDNA, whereas shPafah1b3-2 and shPafah1b3-3 target the 3'UTR of *Pafah1b3* and cannot knockdown the *Pafah1b3* cDNA. (c) Scatterplot showing fold change in shPafah1b3-expressing cells before and after dasatinib treatment *in vitro* in the absence (left) or presence (right) of *Pafah1b3* cDNA. The *Pafah1b3* cDNA rescues the effect of shPafah1b3-2, indicating that its depletion in dasatinib treated cultures is not due to loss of the *Pafah1b3* gene but rather is the result an off-target effect of the hairpin. (d) Scatterplots showing fold change in shRNA-expressing cells in cells

that are either wild-type (left) or express a non-targetable *Pafah1b3* cDNA (right) in co-culture with bone-marrow derived stromal cells. Fold changes are normalized to a hairpin targeting Renilla luciferase. *Pafah1b3* knockdown cells enrich after dasatinib treatment regardless of the presence of a non-targetable *Pafah1b3* cDNA. Percentages are an average of at least three replicates. Error bars represent standard error of the mean; p-values were calculated using Student's t-test.

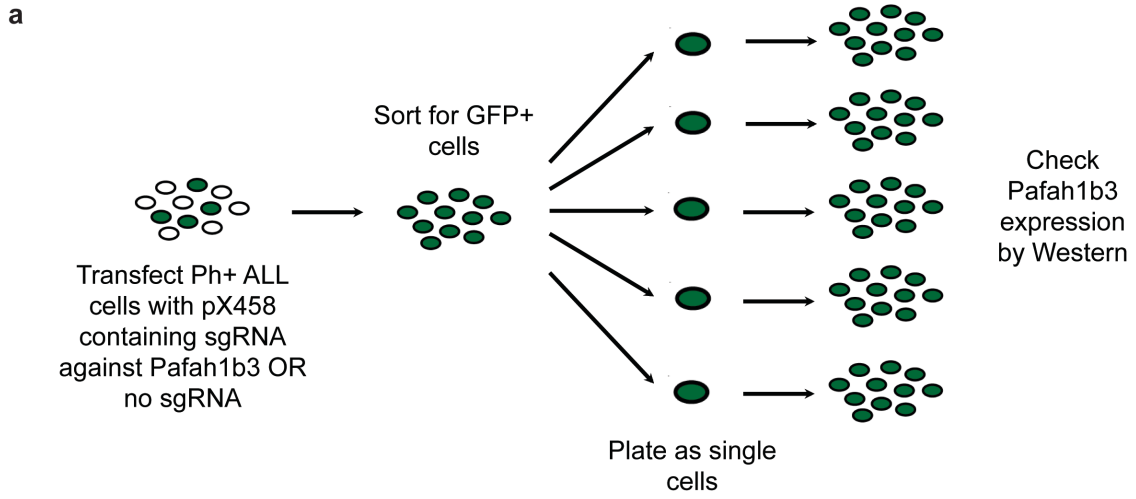

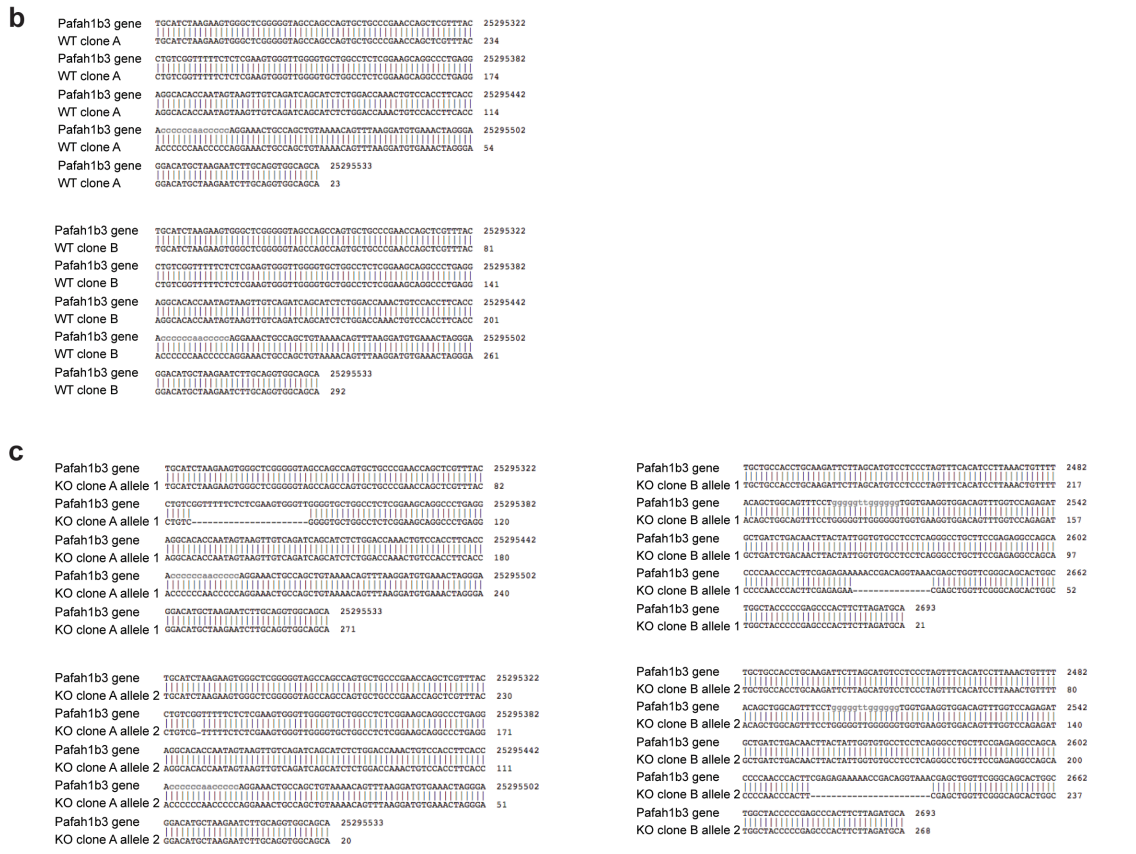

Supplemental Figure S9. CRISPR/Cas9 mediated knockout of Pafah1b3. (a) Schematic of generation of clonal populations of *BCR-ABL1*+ BCP-ALL cells with *Pafah1b3* WT or KO. Leukemia cells are transfected with either empty pX458 vector or pX458 containing an sgRNA targeting the *Pafah1b3* gene, and 24 hours later cells are sorted for the presence of the pX458 construct by using GFP as a marker. pX458 containing cells are then plated out to single cell clones, and once clones have grown out Westerns are performed to check for the presence of Pafah1b3 protein, and Sanger sequencing of the targeting region is performed on (b) wild-type (pX458) and (c) knockout (pX458 + sgPafah1b3) clones.

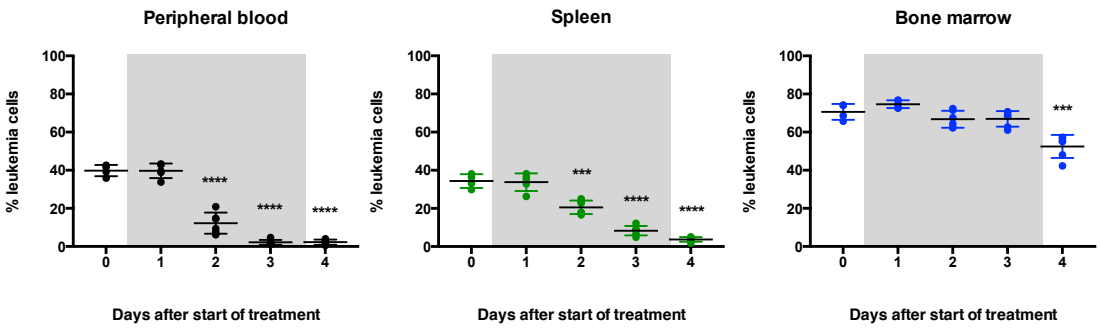

Supplemental Figure S10. Leukemia burden of BCR-ABL1+ BCP-ALL cells is maintained in bone marrow during dasatinib treatment better than in other organs. Scatterplots showing absolute % leukemia cells as assessed by flow cytometry in peripheral blood, spleen, and bone marrow before, during, and after dasatinib treatment. Mice were transplanted with 10^6 GFP+ *BCR-ABL1*+ BCP-ALL cells and treated with 20 mg/kg dasatinib for 3 days q.d. starting at 11 days post-transplant. The grey rectangle indicates the time of treatment. Each timepoint shows data from individual mice. At least 3 mice were used/timepoint. Error bars indicate standard deviation; p-values were calculated using Student's t-test.

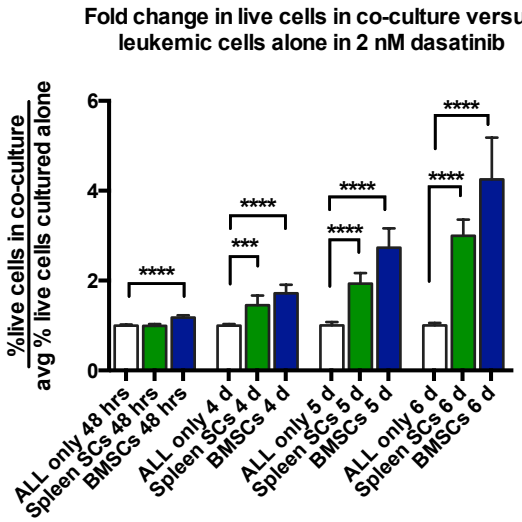

Supplemental Figure S11. Co-culture of BCR-ABL1+ BCP-ALL cells with BMSCs protects from dasatinib mediated cell death. Bar graph showing the percentage of live *BCR-ABL1*+ BCP-ALL cells when co-cultured with bone marrow-derived or spleen-derived stromal cells (BMSCs, blue, or Spleen SCs, green), as assessed by flow cytometry utilizing DAPI staining to determine % live cells. Percentages are normalized to the % live cells of leukemia cells cultured alone (ALL only, white). Cells were plated in 2 nM dasatinib and viability was assessed from the same plates at multiple time points after the start of treatment. Error bars indicate standard deviation; p-values were calculated using Student's t-test.

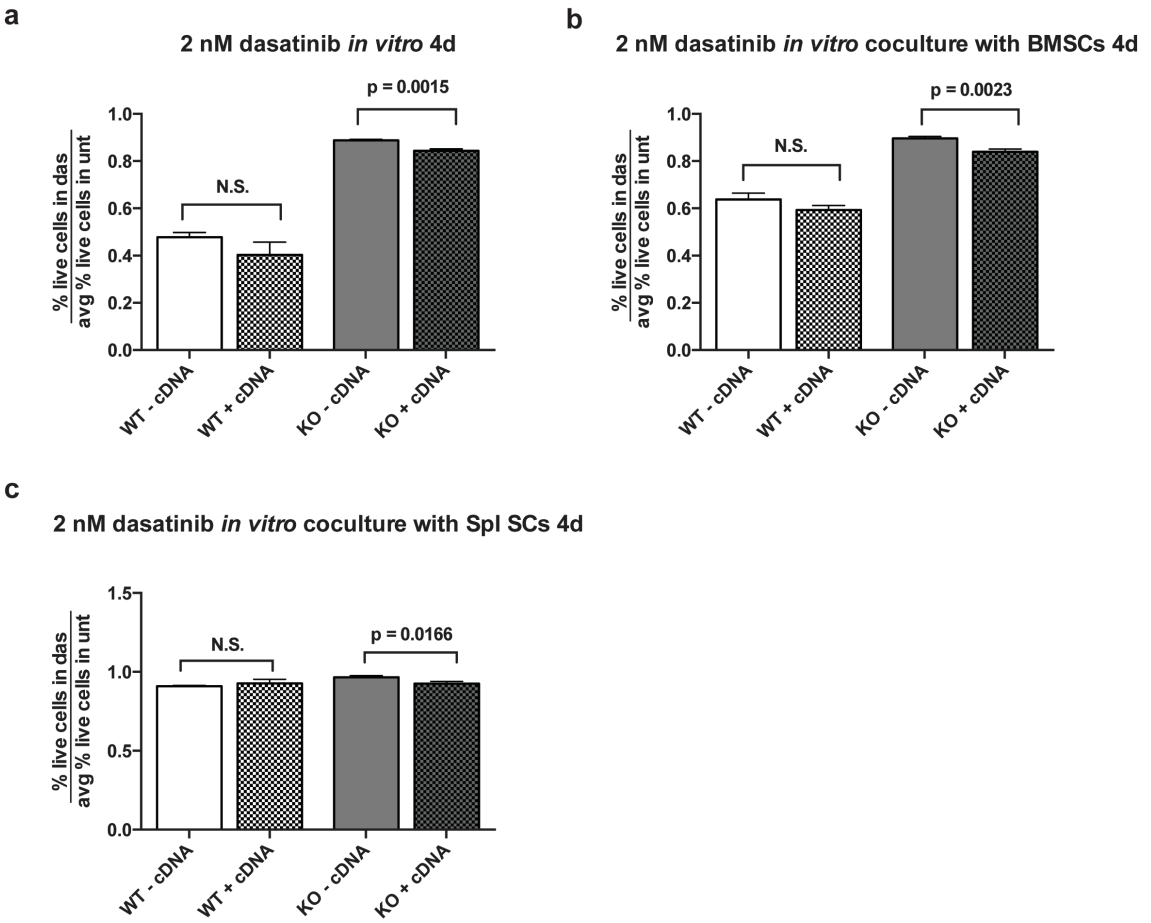

Supplemental Figure S12. Pafah1b3 loss does not result in increased apoptosis after dasatinib treatment in vitro. (a), (b), and (c) Bar graphs showing percentage of live cells in 2 nM dasatinib-treated cultures normalized to percentage of live cells, as assessed by flow cytometry utilizing DAPI staining, in untreated cultures after 4 days of treatment of (a) leukemia cells alone, (b) co-cultured with bone marrow-derived stromal cells, and (c) co-cultured with spleen-derived stromal cells. *Pafah1b3* loss does not result in increased cell death after dasatinib regardless of the presence of stroma. Percentages are an average of three replicates. Error bars for bar graphs indicate standard error of the mean.

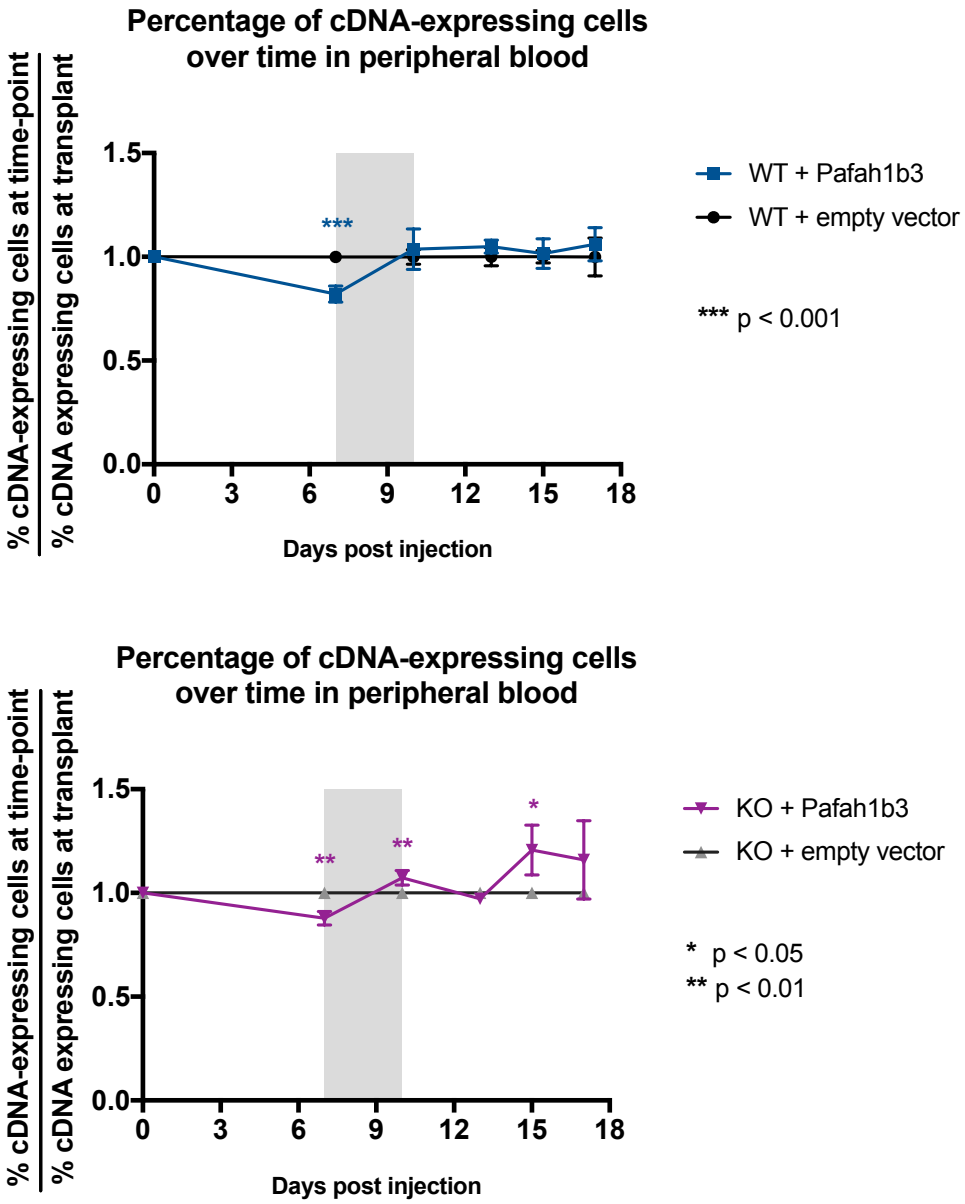

Supplemental Figure S13. Cells over-expressing Pafah1b3 enrich in the peripheral blood on a KO background immediately after therapy. Plot showing the fold change in percent *Pafah1b3* cDNA-expressing cells over time in the peripheral blood of mice receiving transplants of either *Pafah1b3* wild-type or *Pafah1b3* KO cells partially transduced with a *Pafah1b3* cDNA. An empty MSCV vector is used as a control, and the fold change of cDNA-expressing cells is normalized to control. Each time point is an average of 3 - 4 mice that were sacrificed at that time point; this is not longitudinal data. The grey rectangle indicates the time period in which mice were treated with dasatinib. Error bars represent standard deviation.

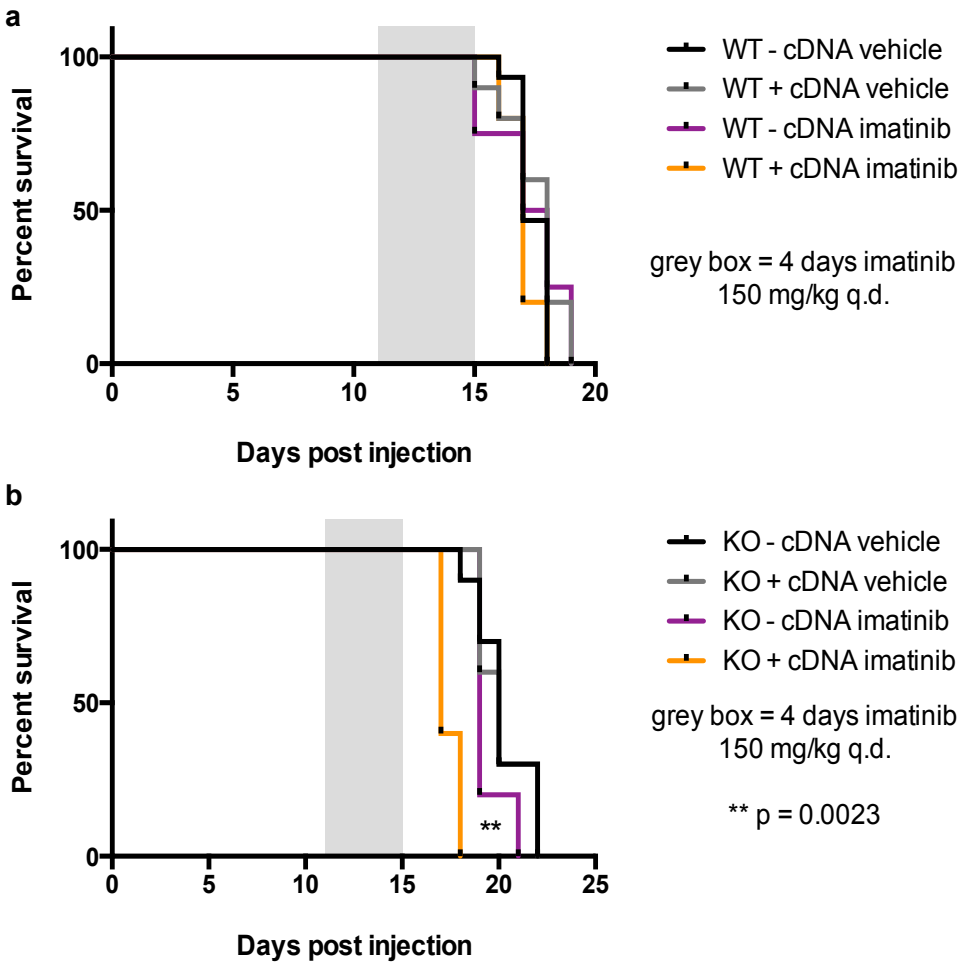

Supplemental Figure S14. Pafah1b3 loss sensitizes BCR-ABL1+ BCP-ALL cells to imatinib treatment in vivo. (a) and (b) Survival analysis of imatinib-treated mice receiving 10^4 WT -cDNA or WT +cDNA cells (a) or KO -cDNA or KO +cDNA cells (b). Imatinib does not extend lifespan in this model, but loss of *Pafah1b3* slightly sensitizes cells to imatinib *in vivo*. Significance was calculated using the Mantel-Cox test; the grey rectangle indicates the time period (4 days q.d., starting at 11 days post-injection) over which imatinib was administered at 150 mg/kg. Five mice were used per condition.

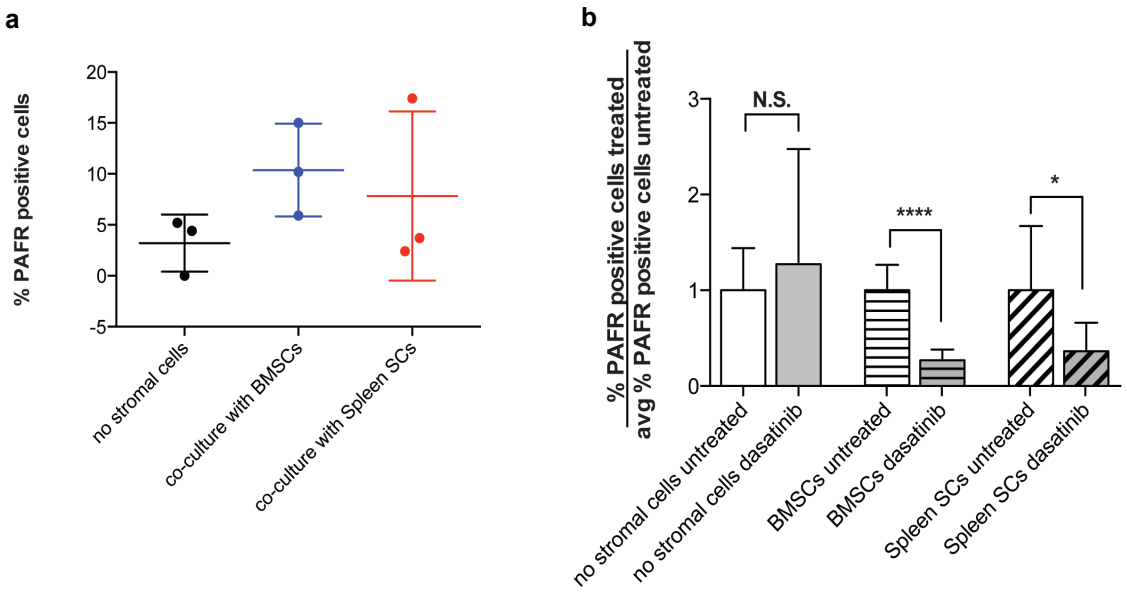

Supplemental Figure S15. Murine p19$^{ARF-/-}$ BCR-ABL1+ BCP-ALL cells express platelet activating factor receptor (PAFR) on the cell surface. (a) Scatterplots showing percentage of leukemia cells expressing PAFR on the cell surface when cultured alone or with bone marrow- of spleen-derived stroma cells. There is a nonsignificant increase in membrane expression of PAFR when leukemia cells are co-cultured with stroma. (b) Bar graphs showing percentage of leukemia cells expressing membrane PAFR when cultured in dasatinib normalized to the percentage of untreated cells expressing membrane PAFR. When leukemia cells are co-cultured with bone marrow- or spleen-derived stromal cells, treatment with dasatinib results in a significant decrease of the percentage of cells expressing membrane PAFR. Error bars represent standard deviation; p-values were calculated using Student's t-test.

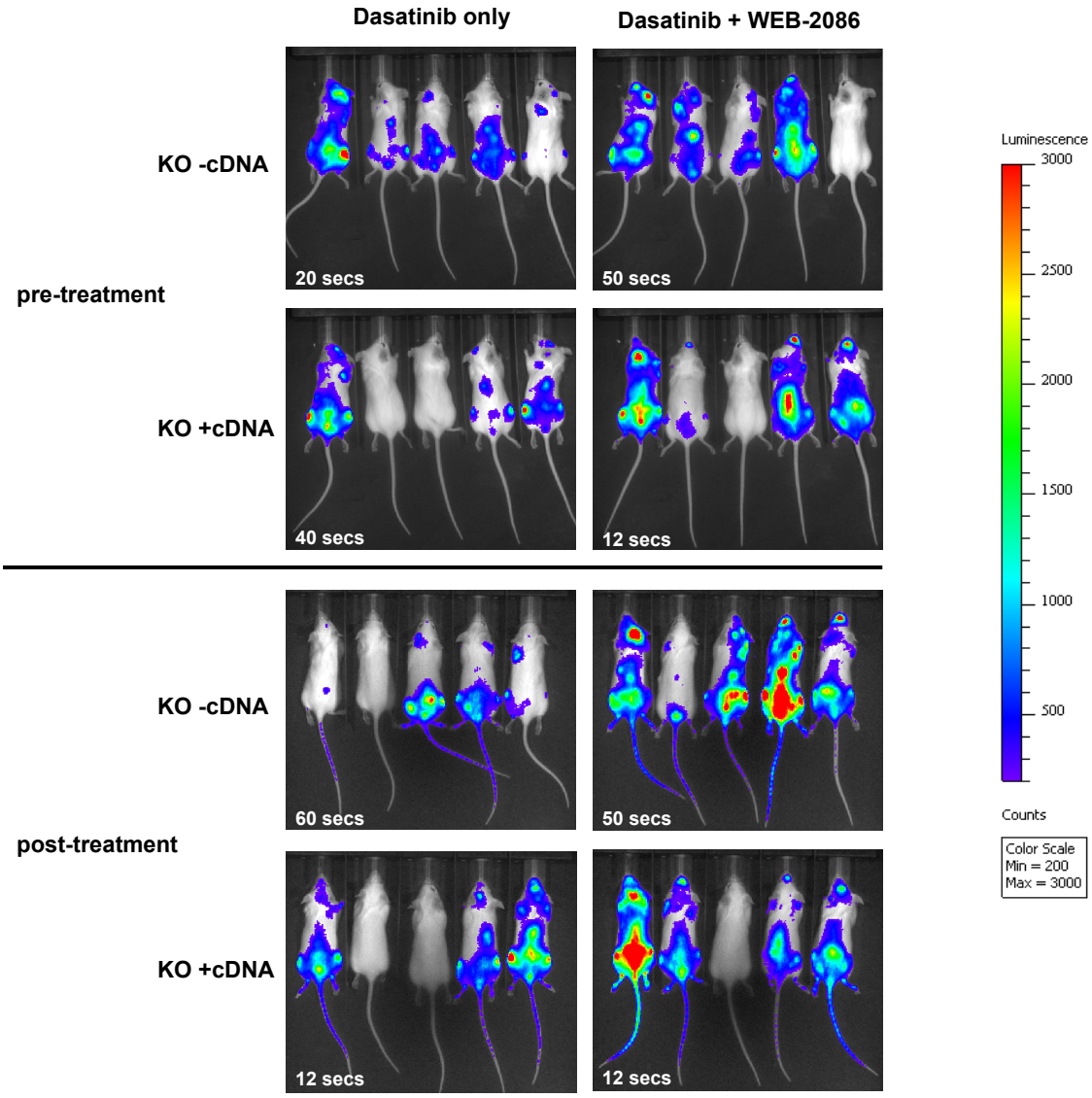

Supplemental Figure S16. In vivo bioluminescent imaging of leukemia burden in mice transplanted with Pafah1b3 KO -/+cDNA and treated with dasatinib and the PAFR antagonist WEB-2086. Representative images of KO-/+cDNA mice receiving either dasatinib alone or dasatinib + WEB-2086 at pre-treatment (11 days post-injection), or post-treatment (14 days post-injection). Pre- and post-treatment refer to timing of dasatinib therapy. Images are shown with the same color scale, but duration of exposure varies and is noted at the bottom left of each image. Several KO+cDNA mice (2nd and 3rd from left in dasatinib alone and middle in dasatinib + WEB-2086) from these images lack detectable burden both before and after dasatinib treatment over multiple different exposure durations and thus are excluded from downstream analyses. Bioluminescent images were collected using a Xenogen IVIS system and analyzed using Living Image version 4.4 software (Caliper Life Sciences).